











Original Article
Biotechnology



In vivo multiplex gene targeting with *Streptococcus pyogenes* and *Campylobacter jejuni* Cas9 for pancreatic cancer modeling in wild-type animal

Yoo Jin Chang ^{1,2}, Jihyeon Bae ¹, Yang Zhao ¹, Geonseong Lee ¹,
Jeongpil Han ¹, Yoon Hoo Lee ¹, Ok Jae Koo ³, Sunmin Seo ⁴,
Yang-Kyu Choi ⁴, Su Cheong Yeom ^{1,5,*}

¹Graduate School of International Agricultural Technology, Seoul National University, Pyeongchang 25354, Korea

²Department of Pharmacology, Yonsei University College of Medicine, Seoul 03722, Korea

³Toolgen Inc., Seoul 08594, Korea

⁴Department of Laboratory Animal Medicine, College of Veterinary Medicine, Konkuk University, Seoul 05029, Korea

⁵Designed Animal and Transplantation Research Institute, Greenbio Research and Technology, Seoul National University, Pyeongchang 25354, Korea



Received: Jul 23, 2019

Revised: Dec 4, 2019

Accepted: Dec 6, 2019

*Corresponding author:

Su Cheong Yeom

Graduate School of International Agricultural Technology, Seoul National University, 1447 Pyeongchang-daero, Daewha-myeon, Pyeongchang 25354, Korea.
E-mail: scyeom@snu.ac.kr


© 2020 The Korean Society of Veterinary Science

This is an Open Access article distributed under the terms of the Creative Commons Attribution Non-Commercial License (<https://creativecommons.org/licenses/by-nc/4.0>) which permits unrestricted non-commercial use, distribution, and reproduction in any medium, provided the original work is properly cited.


ORCID iDs

Yoo Jin Chang 

<https://orcid.org/0000-0001-5421-3771>

Jihyeon Bae 

<https://orcid.org/0000-0001-6614-5972>




Yang Zhao 

<https://orcid.org/0000-0003-0880-1788>

ABSTRACT

Pancreatic ductal adenocarcinoma is a lethal cancer type that is associated with multiple gene mutations in somatic cells. Genetically engineered mouse is hardly applicable for developing a pancreatic cancer model, and the xenograft model poses a limitation in the reflection of early stage pancreatic cancer. Thus, *in vivo* somatic cell gene engineering with clustered regularly interspaced short palindromic repeats is drawing increasing attention for generating an animal model of pancreatic cancer. In this study, we selected *Kras*, *Trp53*, *Ink4a*, *Smad4*, and *Brca2* as target genes, and applied *Campylobacter jejuni* Cas9 (CjCas9) and *Streptococcus pyogenes* Cas9 (SpCas9) for developing pancreatic cancer using adeno associated virus (AAV) transduction. After confirming multifocal and diffuse transduction of AAV2, we generated SpCas9 overexpression mice, which exhibited high double-strand DNA breakage (DSB) in target genes and pancreatic intraepithelial neoplasia (PanIN) lesions with two AAV transductions; however, wild-type (WT) mice with three AAV transductions did not develop PanIN. Furthermore, small-sized Cjcas9 was applied to WT mice with two AAV system, which, in addition, developed high extensive DSB and PanIN lesions. Histological changes and expression of cancer markers such as Ki67, cytokeratin, Mucin5a, alpha smooth muscle actin in duct and islet cells were observed. In addition, the study revealed several findings such as 1) multiple DSB potential of AAV-CjCas9, 2) peri-ductal lymphocyte infiltration, 3) multi-focal cancer marker expression, and 4) requirement of > 12 months for initiation of PanIN in AAV mediated targeting. In this study, we present a useful tool for *in vivo* cancer modeling that would be applicable for other disease models as well.

Keywords: Adeno-associated virus; CRISPR; gene editing; Pancreatic cancer

Geonseong Lee <https://orcid.org/0000-0001-7715-3687>Jeongpil Han <https://orcid.org/0000-0003-2057-0820>Yoon Hoo Lee <https://orcid.org/0000-0002-4430-0895>Ok Jae Koo <https://orcid.org/0000-0001-6399-6472>Sunmin Seo <https://orcid.org/0000-0001-7543-846X>Yang-Kyu Choi <https://orcid.org/0000-0002-4969-5443>Su Cheong Yeom <https://orcid.org/0000-0002-9491-5740>

Funding

This work was supported by grant from the National Research Foundation (Nos. NRF-2015R1C1A1A01051949, 2017M3A9B4061409 and 2018R1A1A1A05078158).

Conflict of Interest

The authors declare no conflicts of interest.

Author Contributions

Conceptualization: Chang YJ, Yeom SC; Formal analysis: Chang YJ, Bae J, Zhao Y, Lee G, Han J, Lee YH, Seo S, Choi YK; Writing - original draft: Chang YJ, Yeom SC; Writing - review & editing: Chang YJ, Yeom SC.

INTRODUCTION

Pancreatic ductal adenocarcinoma (PDAC) is one of the most lethal cancer types, and is associated with rapid degeneration and resistance to treatment. Because the symptoms are nearly imperceptible, the disease eludes detection period, which leads to a 5-year survival rate of $\leq 5\%$. The exact etiology of pancreatic cancer is not known; however, risk factors include smoking and nonhereditary chronic pancreatitis [1]. Pancreatic cancer originates in several cell types, but pancreatic ductal intraepithelial cells are commonly affected at the outset of PDAC [2]. Normally, spontaneous somatic cell mutation develops into cancer, and most frequently mutated genes in pancreatic cancer are *Kras*, *Ink4a*, *Tp53*, *Smad4*, and *Brca2* [2,3]. Each of gene plays a role in the developmental stage of pancreatic intraepithelial neoplasia (PanIN), which classified into PanIN-1, PanIN-2, PanIN-3, and PDAC [4].

A pancreatic cancer animal model could provide opportunities for preclinical studies, and understanding complex gene interactions and pathological progression. PDAC animal models have been established with syngeneic tumor graft, human tumor cell-line xenograft, genetically engineered mice (GEM), and patient derived cell xenograft [5]. The xenograft model offers advantages like mimicking genetic and epigenetic abnormality and reproducibility of microenvironment as tumor itself [6], but has a limitation in the reflection of early stage PDAC development. PDAC GEM model could be applied to study cancer biology and its progression and many types of PDAC GEM models have been generated through *Kras*^{G12D} mutations and conditional knock-out systems [7]. Nevertheless, they are hardly applicable, time-consuming, and laborious. which remains the current studies about pancreatic cancer to be localized in *in vitro* level.

Recently discovered clustered regularly interspaced short palindromic repeats (CRISPR)/Cas9 is an adaptive defense system in prokaryotic cells, which emerged as a powerful and efficient tool for gene manipulation in eukaryotic cells and embryos [8]. With high potential for site-specific double strand breakage (DSB), CRISPR/Cas9 can be used to perform simultaneous and multiplex gene editing in the embryo [9]; however, CRISPR mediated PDAC animal generation is hardly applicable as several PDAC related genes cause embryonic lethality [10]. Besides, pancreatic cancer GEM model just reflects familial PDAC, but common cause of PDAC is spontaneous somatic cell mutation in the acini cells or pancreatic duct. Thus, *in vivo* somatic cell gene engineering with CRISPR has been receiving attention for generation of cancer in various organs including the lung, liver, brain, retina, and pancreas [11-16]. Even technical advances have been made in *in vivo* PDAC modeling, but a model could be developed based on pre-established Cas9 overexpression, *Kras*^{LSL-G12D} or *p53*^{LSL-R172H} mice [15,17].

In this study, we applied two different CRISPR/Cas9 orthologues such as *Streptococcus pyogenes* Cas9 (SpCas9) and *Campylobacter jejuni* Cas9 (CjCas9) for *in vivo* and multiplex somatic cell gene mutations. First, we aimed to develop SpCas9 overexpression mice, and evaluated DSB potential of single guide RNAs (sgRNAs) and adeno associated virus (AAV) tropism in the pancreas. Finally, AAV packed with Cas9 were transduced into the pancreas via the common bile duct and evaluated for DSB frequency and pancreatic cancer development.

MATERIALS AND METHODS

Animals

C57BL/6 (B6) and FVB mice were purchased from Koatech (Korea), and C57BL/6.TgTn (pb-CAG-SpCas9/RFP) (B6.SpCas9) was produced by in-house generation. All mice were maintained under SPF grade with *ad libitum* access to water and food. This study was approved by the Institutional Animal Care and Use Committees of Seoul National University (SNU-160913-2) and was conducted in accordance with the approved guidelines.

Designing of sgRNA and HDR template

Among PDAC related genes, *Kras*, *Ink4a1*, *Cdkn2a-ex1β*, *Tp53*, *Smad4* and *Brca2* were selected as targets [2,18]. In addition, SpCas9 and CjCas9 were applied for gene editing. In order to modify *Kras*^{G12D} substitution, sgRNAs were designed in adjacent site of 12th codon according to orthologue specific PAM sequence as 5'-NGG-3' in SpCas9 and 5'-NNNNRYAC-3' in CjCas9. Donor templates were prepared with homology arms and silent mutations were done to prevent re-cutting by CRISPR. With relatively high frequency of PAM sequence of SpCas9, sgRNA binding site could cover target region, so just one sgRNA and small number of silent mutations could be applicable. sgRNA binding site for CjCas9 is far from target site; thus, two different sgRNAs and relatively many number of silent mutations was needed in homology directed repair template. For loss of function gene editing, same sgRNA sequences with previous report were used in SpCas9 [16], and sgRNA sequences for CjCas9 were determined by *in silico* designing with 22 base pair sgRNA binding sequences [19]. Targeting map and all sgRNA sequences are listed in **Supplementary Fig. 1** and **Supplementary Table 1**.

DSB potential evaluation of sgRNAs

After cloning AAV-CRISPR plasmids as **Fig. 1A**, DSB potentials of each sgRNA were evaluated using embryos. 50 ng/μL of AAV-SpCas9 and 15 ng/μL AAV-3 sgRNA plasmid and AAV-CjCas9-3 sgRNA were microinjected into one-cell stage embryos and cultured till the blastocyst stage. After polymerase chain reaction (PCR) for each target, amplicons were subjected to hetero-duplex formation, followed by running on an sodium dodecyl sulfate-polyacrylamide gel electrophoresis gel. DSB potential was estimated with the existence of unspecific fragment by comparing with wild-type (WT) [20]. Primer sequences in this study are listed in **Supplementary Table 2**.

Generation of SpCas9 overexpression mice with PiggyBac transposon system

Plasmid vector harboring ITR-CAG promoter-SpCas9/RFP-PuroR-pA-ITR (pPB-SpCas9/RFP) was synthesized (**Fig. 1B**). Next, one-cell stage embryos were obtained after pregnant mare's gonadotropin (Prospec Bio, USA) and human chorionic gonadotropin (Prospec Bio) injection and followed by microinjection into pronucleus with PB-SpCas9/RFP and transposase plasmid. After embryo transfer into the oviduct of recipient foster dams, the produced pups were genotyped via PCR.

Analysis of AAV2 tropism in the pancreas

In order to identify AAV2 tropism in pancreas ductal epithelial cell, 1.29×10^{10} MOI of AAV-enhanced green fluorescent protein (eGFP) was injected into pancreas via common bile duct. Briefly, after anesthetizing, dissection was performed on the lower abdomen and diaphragm, the duodenum was gently pulled over and was covered with wet gauze for preventing dry, and AAV was injected into sphincter of oddi under the microscope with a 30-gauge needle after placing

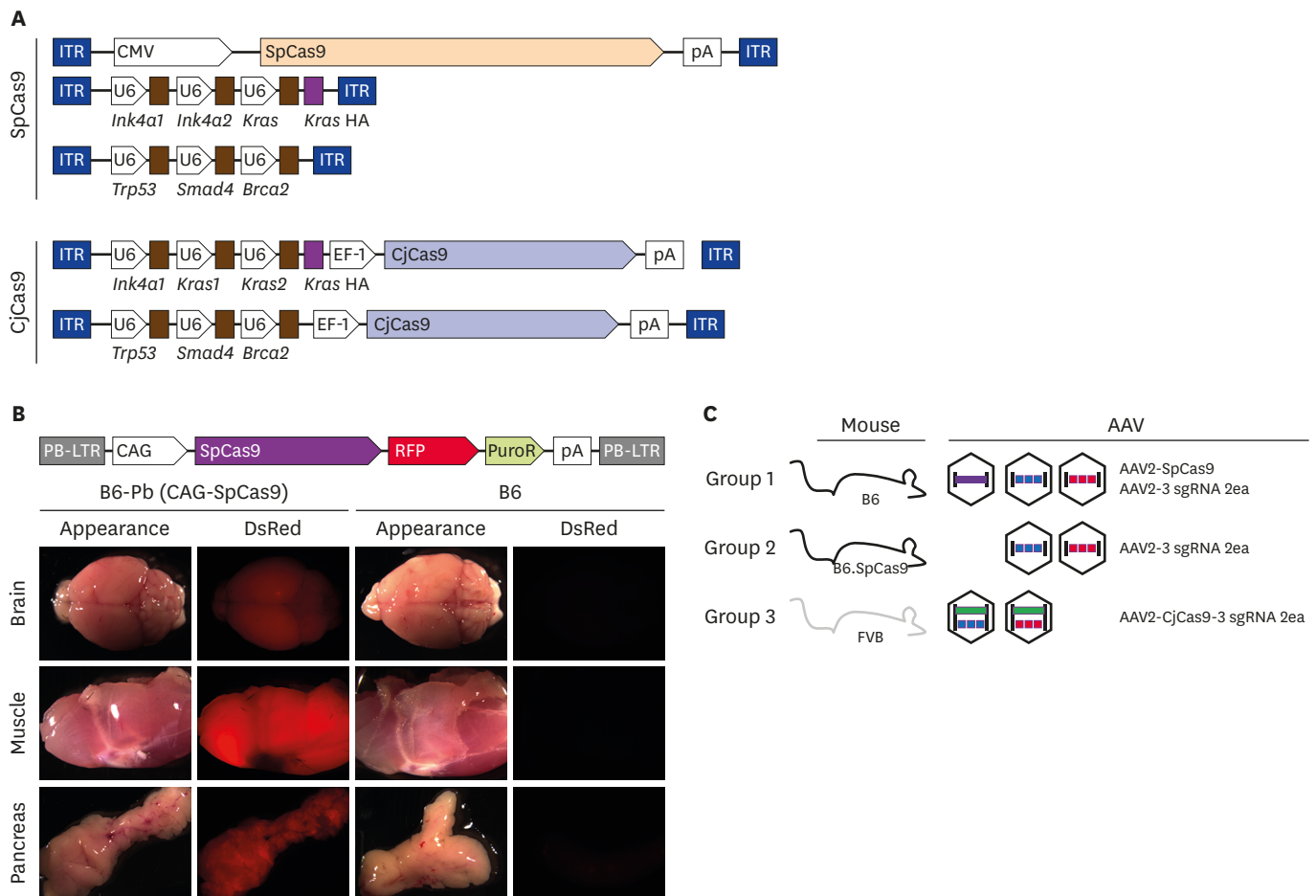


Fig. 1. Brief schematic of *in vivo* gene targeting with CRISPR/Cas9 (A) Vector maps of AAV-SpCas9, AAV-3 sgRNA, and AAV- CjCas9-all-in-one used in this study. Five different rAAV vectors were prepared by synthesis and cloning. Blue box: ITR sequence from AAV2, arrow box: promoter, brown box: sgRNA sequence. (B) SpCas9 overexpression mouse generation with PiggyBac transposon system. pCAG-SpCas9-RFP-pA insert was incorporated into host genome by transposase. Gene integration confirmed by RFP expression under stereoscope microscope. (C) Experimental group of *in vivo* gene targeting for pancreatic cancer development. WT C57BL/6 mice were injected with three AAVs; AAV2-SpCas9, AAV2-3 sgRNA (*Kras-Ink4a1-Ink4a2*-HA) and AAV2-3 sgRNA (*Trp53-Smad4-Brca2*) into common bile duct in group 1. Instead of AAV2-SpCas9 injection, SpCas9 overexpression mice were applied in group 2. WT FVB mice and all-in-one type two AAVs (AAV2-CjCas9-sgRNA for *Kras*, *Ink4a*-HA and AAV2-CjCas9-sgRNA for *Trp53*, *Smad4*, *Brca2*) were injected in group 3. Detailed information of each target is provided in **Supplementary Fig. 1** and **Supplementary Table 1**. AAV, adeno associated virus; SpCas9, *Streptococcus pyogenes* Cas9; CjCas9, *Campylobacter jejuni* Cas9; sgRNA, single guide RNA; CRISPR, clustered regularly interspaced short palindromic repeats; rAAV, recombinant adeno associated virus; WT, wild-type.

microclip close to cystic duct [15]. After 3 and 7 weeks from AAV-eGFP injection, GFP signal on pancreas region was detected with fluorescence stereo-microscopes (Leica, Germany).

Recombinant AAV (rAAV) preparation

Vector for AAV2-CMV-SpCas9-pA (pAAV-SpCas9), AAV2-3 U6 and sgRNAs (pAAV-3 sgRNA), and AAV2-EF1-CjCas9-pA-3 U6 and sgRNAs (pAAV-CjCas9-3 sgRNA) were prepared for rAAV production. In house rAAVs production was conducted with AAVpro helper free system (Takara, Japan) according to the manufacturer's instruction. Briefly, each plasmid of AAV-SpCas9, AAV-3 sgRNA and AAV-CjCas9-3 sgRNA were co-transfected into HEK293 cells with helper and AAV2 specific Rep/cap plasmid using calcium phosphate transfection method and cultured for 4 days in 2% fetal bovine serum and 5% CO₂. After AAV purification with commercial kit, quantitative PCR based titration was conducted with primers located in the inverted terminal region and stored at -80°C until use.

In vivo transduction with AAVs-SpCas9 and AAV-CjCas9 in the pancreas

Five-weeks-old B6, B6.SpCas9 and FVB mice were subjected to AAV transduction. 2.6×10^{10} of AAV-SpCas9 and 2 different AAV-3 sgRNAs (*Ink4a1-Ink4a2-Kras* and *Trp53-Smad4-Brca2*) with 1.3×10^{10} viral particle were transduced into B6 mice as group 1. B6.SpCas9 mice were used as group 2, and only 1.3×10^{10} viral particle of 2 types AAV-3 sgRNA were transduced. Group 1 and 2 utilized SpCas9 orthologue with B6 background mice, group 3 used CjCas9 orthologue with FVB mice, and 2 types all-in-one type AAV-CjCas9-3 sgRNA (*CjCas9-Ink4a-Kras1-Kras2* and *CjCas9-Trp53-Smad4-Brca2*) were applied with 1.3×10^{10} viral particle (**Fig. 1C** and **Supplementary Table 2**). The same volume of saline was injected into the pancreas in B6, B6.SpCas9 and FVB for control (n = 5 per each group).

Sequencing for indel and SNP detection in target genes

After 6 and 12 months of AAV transduction, pancreatic tissues were homogenized with glass-bead and genomic DNA was extracted by conventional phenol-chloroform method. In order to analyze insertion/deletion (indel) frequency, PCR amplicons for each target were applied to Sanger sequencing and analyzed with software algorithm of Synthego ICE tool (<https://ice.synthego.com>) [21]. Primers used in this study are listed in **Supplementary Table 3**.

Histological examination for cancer development

Formalin fixed pancreas tissues used for hematoxylin and eosin (H&E) staining and immunohistochemistry (IHC) analysis. In H&E staining, deparaffinized tissues were stained with 0.1% of Mayer's H&E solution. In IHC, slides were blocked with control serum, followed by primary and secondary antibodies incubation and signal detection. Briefly, rabbit anti-mouse antigen KI-67 (Ki67), pan-cytokeratin, Mucin5 α and alpha smooth muscle actin (α SMA) (Biorbyt, USA) was used for primary antibodies and Vectastain ELITE ABC kit with diaminobenzidine (Vectorlaboratories, USA) was used for detection.

RESULTS

SpCas9 overexpression mice was produced by PiggyBac system

In order to develop *in vivo* gene modifications in the five genes, we applied AAV and two different cas9 orthologues. In addition, viruses such as AAV, adenovirus and lentivirus have been applied to develop somatic cell *in vivo* gene editing [12,15]. AAV is the most widely utilized virus for *in vivo* gene editing but it has approximately 4.7 kbp cargo capacity limitation [22], and large-sized CRISPR orthologue such as SpCas9 cannot be packed into AAV together with sgRNA producing sequence, thus splitting it into two parts as AAV-SpCas9 and AAV-sgRNA is commonly utilized [23,24]. Owing to this reason, three AAV vectors were needed for SpCas9, but just two AAV vectors for CjCas9 (**Fig. 1A and C**). As multiple co-delivery would be less efficient in AAV-CRISPR mediated *in vivo* gene modification, we tried to generate SpCas9 overexpression mice with PiggyBac system. As expected, B6.SpCas9 exhibited high RFP signal expression in the pancreas, brain, and muscles (**Fig. 1B**), and was applied to further *in vivo* AAV-SpCas9 transduction for the pancreas.

SpCas9 and CjCas9 exhibited high DSB potential in target genes

In DSB potential analysis with SpCas9-sgRNA, PCR and hetero-duplex PAGE assay on genomic DNA extracted from blastocysts of microinjected embryos revealed various cleavage efficiencies by the genes, which are *Kras* (87.5%, 7/8), *Ink4a1* (*CdKn2a-ex1 β*) (75%, 6/8), *Ink4a2* (*CdKn2a-ex2*) (75%, 6/8), *Trp53* (25%, 2/8), *Smad4* (37.5%, 3/8), and *Brca2* (12.5%, 1/8) (**Fig. 2A**).

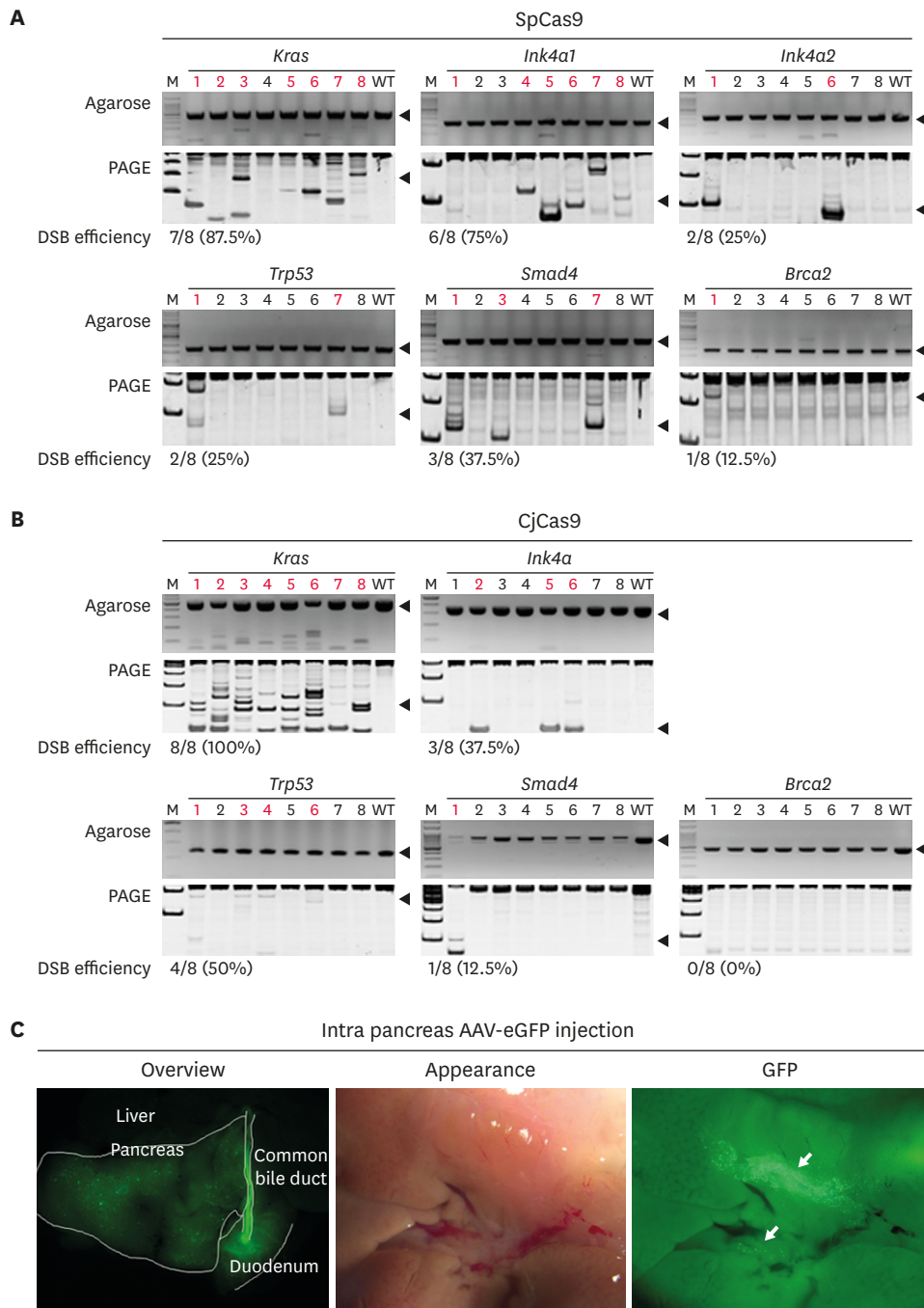


Fig. 2. Evaluation of DSB efficiency and AAV2 tropism in pancreas (A) and (B). Cas9 messenger RNA and 3 single guide RNAs plasmid were co-injected into 1 cell stage embryos and DSB was evaluated by hetero-duplex formation and SDS-PAGE gel. Red letters indicate DSB and black arrow indicates the target size of each polymerase chain reaction. DSB efficiency presented as number of embryos with DSB/number of total embryos used (%). (C) After 3 weeks of AAV2-eGFP injection into pancreas, GFP expression analyzed with stereoscopic microscope. White guideline distinguishes each of the organs and white arrows indicates spots for GFP expression. Statistical analysis was performed using Student's *t*-test.

SpCas9, *Streptococcus pyogenes* Cas9; CjCas9, *Campylobacter jejuni* Cas9; DSB, double-strand DNA breakage; SDS-PAGE, sodium dodecyl sulfate-polyacrylamide gel electrophoresis; AAV, adeno associated virus; eGFP, enhanced green fluorescent protein; GFP, green fluorescent protein; WT, wild-type.

Further, DSB potential analysis for CjCas9 presented as *Kras* (100%, 8/8), *Ink4a2* (*CdKn2a-ex2*) (37.5%, 3/8), *Trp53* (50%, 4/8), *Smad4* (12.5%, 3/8), and *Brca2* (0%, 0/8) gene (**Fig. 2B**). Even

CjCas9 in *Brca2* could not develop DSB in the embryo; overall, DSB potential seemed to be high enough for application of further *in vivo* gene editing.

AAV2 showed tropism in pancreatic duct

One of the ultimate conditions for successful *in vivo* gene targeting is to deliver a gene directly into the target organ or specific cells. AAVs exhibit serotype dependent tropism [22]; serotype selection and tropism validation are an important factor for AAV mediated *in vivo* transduction. Because AAV2 has diverse tissue tropism and is easily obtained by in-house rAAV production [22], we selected AAV2 as the target serotype for *in vivo* gene editing in the pancreas. Next, AAV2 tropism in pancreas with C57BL/6 and FVB was confirmed with directly injecting GFP packaging AAV into the common bile duct of the pancreas. GFP signal was higher at 3 weeks than 7 weeks after AAV transduction, and signal intensity remarkably decreased at 7 weeks (**Supplementary Fig. 2**). In detail, the GFP signal was highly expressed in the common bile duct and adjacent duct; in addition, it was detected in the entire region of the pancreas with a diffuse and multi-focal pattern. The reason of high GFP signal expression in the common bile duct is uncertain, but it might be caused by transduction during injection, or under clearance after GFP synthesis in the transduced pancreas cell. Nevertheless, no GFP expression in the liver suggests that our pancreatic injection method was applicable in local pancreatic injection. Taken together, AAV2 could survive and produce protein for several weeks in the pancreas, and injection into common bile duct is applicable for pancreatic duct specific AAV transduction (**Fig. 2C** and **Supplementary Fig. 2**).

AAV-CRISPR developed DSB and SNP in the pancreas

Since it was difficult to separate only the tumor tissue, the indel frequency was analyzed using DNA of the whole pancreas tissue. In the *Trp53* gene, group 1 mice exhibited no indel, but group 2 mice with the same sgRNA presented approximately 5% indel frequency. Similarly, the *Kras* gene developed relatively higher indel frequency in group 2 mice than group 1 mice. This suggests that SpCas9 overexpression mice are better than WT for *in vivo* gene editing. This might be caused by a limitation on simultaneous transduction of 2 different AAVs into the same cells, but endogenous SpCas9 expression in group 2 mice gave an advantage for this. In addition, even SpCas9 showed relatively high DSB formation potential in embryos (**Fig. 2A and B**), but CjCas9 exhibited higher DSB frequency than SpCas9 in *Trp53* and *Kras* at *in vivo* gene editing. The other target genes such as *Brca2* and *Smad4* did not develop high DSB frequency, but *Ink4a* targeting seemed to develop high indel frequency (**Fig. 3A**). On comparison of the indel efficiency between targets in the same AAV vector (*Ink4a-Kras* and *Trp53-Smad4-Brca2*), DSB potential seemed to depend on sgRNA DSB potential than location of the cloning vector. In the additional analysis for *Kras*^{G12D} mutation, mice in all the groups exhibited low frequency of mutation. This SNP and indel frequency seemed to be lower than that recently reported in a study [17]. However, we collected whole pancreatic tissue for analyzing overall gene editing efficiency, but previous studies analyzed genomic DNA from neoplasm tissues, and this difference would probably have led to relatively low *in vivo* targeting efficiency.

AAV-CRISPR induced immune cell infiltration in pancreas

None of the mice exhibited symptoms such as weakness, hunching, or jaundice until 12 months. After 6 months from AAV transduction, histological analysis of pancreatic tissues was performed, but no mice developed remarkable neoplasia formation. However, islet hyperplasia in group 2 mice and lymphoid cell infiltration in group 3 mice were observed (**Fig. 3B** and **Table 1**). Whereas at 12 months after AAV transduction, several abnormal appearances in group 2 and 3

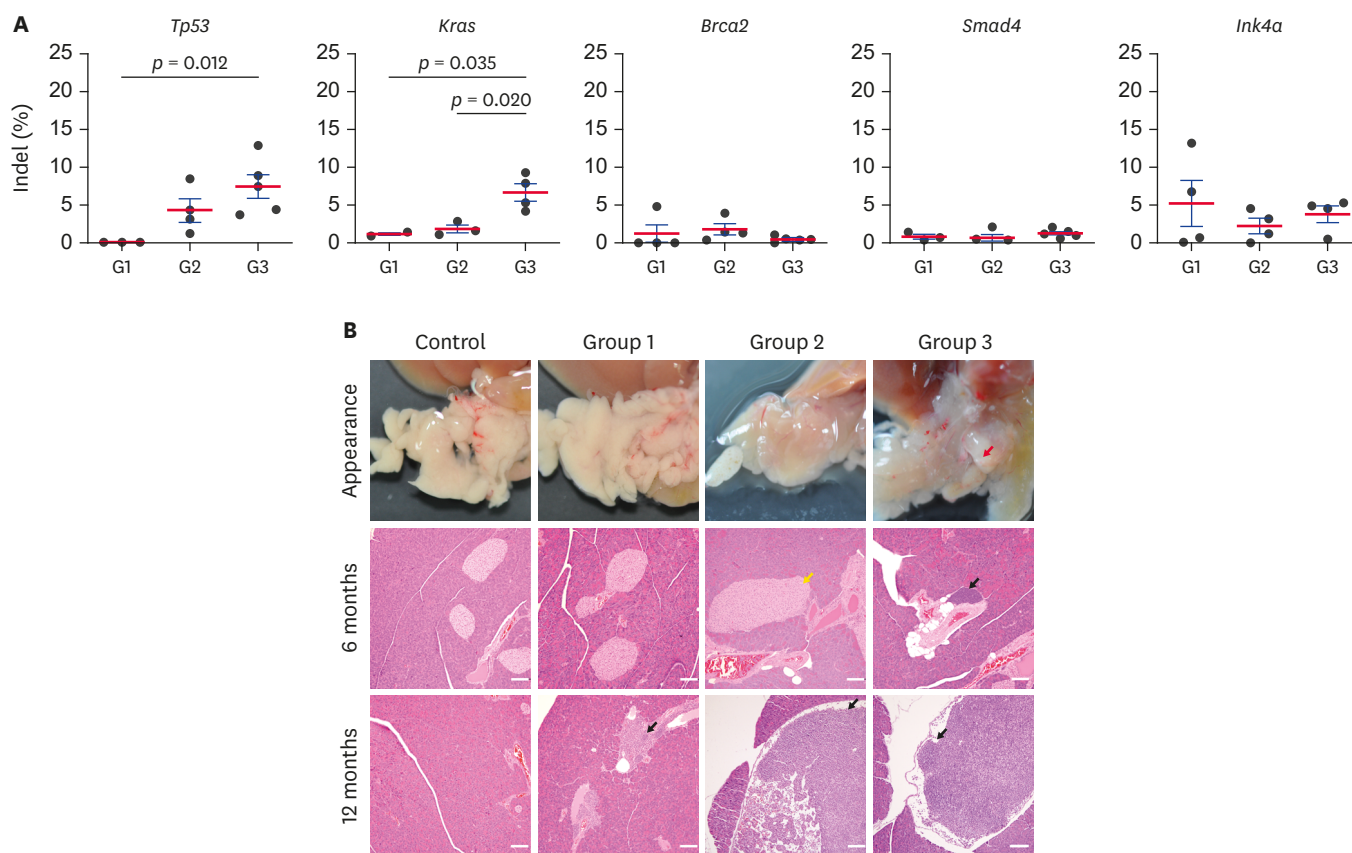


Fig. 3. DSB frequency analysis and macroscopic examination (A) Indel frequency of target genes was analyzed with Sanger sequencing and algorithm of Synthego ICE tool. Each dot indicates DSB rate from each mice. Statistical analysis was performed with Student's *t*-test, and $p < 0.05$ indicated significantly different. (B) Appearance and microscopic analysis on pancreas. Red arrow: abnormal lesion, yellow arrow: islet hyperplasia, black arrow: peri-ductal lymphocyte infiltration and mesentery lymph node, white bar, 200 μ m. DSB, double-strand DNA breakage.

Table 1. Summary of *in vivo* gene targeting for developing pancreatic cancer

Group	Strain	Component	6 (mo)	12 (mo)
Group 1	B6	AAV-SpCas9 AAV- <i>Ink4a1-Ink4a2-Kras-Kras</i> HA AAV- <i>Tp53-Smad4-Brca2</i>	-	Lymphoid cell infiltration Cancer marker expression (α SMA)
Group 2	B6.PB-SpCas9	AAV- <i>Ink4a1-Ink4a2-Kras-Kras</i> HA AAV- <i>Tp53-Smad4-Brca2</i>	Islet hyperplasia	Mesentery lymph node penetration, PanIN, cancer marker expression (Ki67, cytokeratin, Mucin5a, α SMA)
Group 3	FVB	AAV- <i>Ink4a-Kras1-Kras2-Kras</i> HA AAV- <i>Tp53-Smad4-Brca2</i>	Lymphoid cell infiltration	Mesentery lymph node penetration, PanIN, cancer marker expression (Ki67, cytokeratin, α SMA)

AAV, adeno associated virus; SpCas9, *Streptococcus pyogenes* Cas9; α SMA, alpha smooth muscle actin; PanIN, pancreatic intraepithelial neoplasia.

mice were noted. Furthermore, mice in all the groups exhibited severe peri-ductal immune cell infiltration, and this was similar to the previously reports in pancreatic cancer model [25]. A large-sized mass of immune cells, which seemed to be mesenteric lymph node, penetrated the pancreas in group 2 mice. Additionally, the mouse displayed loose dispersed mesenteric pattern pancreas, but fusion and lymph node penetration seemed to be an uncommon finding (Fig. 3B and Supplementary Fig. 3).

AAV-CRISPR induced PanIN after 12 months

Next, we evaluated pancreatic cancer development via microscopic examination. Mice in group 2 and 3 presented pancreatic cancer lesion in the duct. However, cancer lesion was not found

in organs other than pancreas in all groups. In detail, group 2 mice exhibited PanIN with flat and columnar epithelium [4], and expression of cancer markers such as cytokeratin, α SMA, Mucin5a, and Ki67. Group 3 mice also developed remarkable histological changes, and they exhibited PanIN-like lesions and cancer marker expression in the duct area (**Fig. 4A and B**). The α SMA, a marker of pancreatic stellate cell activation [26], exhibited strong expression in ductal epithelial cells of group 2 mice, and slightly high in group 3 mice (**Fig. 4A**). Mucin5a, which is pancreatic cancer marker and has an important role for tumor development, progression, and metastasis [27] also highly expressed in ductal epithelial cells and islet cells in group 2 mice (**Fig. 4A**). Pan-cytokeratin, α SMA and Mucin5a, positive cells were just observed in the ductal

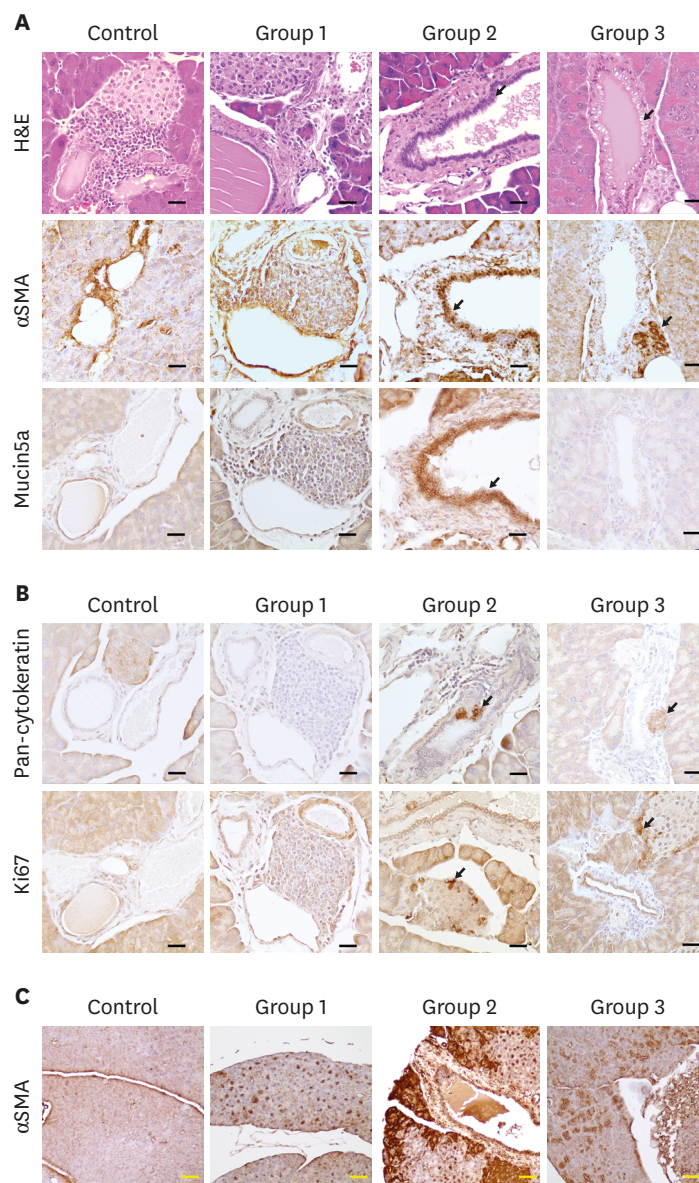


Fig. 4. Histological and IHC analysis for evaluation of pancreatic cancer development (A) and (B) H&E stain and IHC for pan-cytokeratin, α SMA, Mucin5a, and Ki67 was conducted with formalin fixed pancreatic tissues. Black arrow: PanIN lesion or cancer marker expression. Black scale bar: 50 μ m (C) IHC for α SMA marker. Yellow scale bar, 100 μ m.

IHC, immunohistochemistry; α SMA, alpha smooth muscle actin; H&E, hematoxylin and eosin; PanIN, pancreatic intraepithelial neoplasia.

area, but ki67, a marker of cell proliferation and marker of pancreatic neuroendocrine cancer [28], is detected in the margin of islet cells of group 2 and 3 mice (**Fig. 4B**). α SMA and Mucin5a co-expressed at the same epithelial duct site, but the expression of pan-cytokeratin and ki67 was observed at different sites, and this may be due to the difference in characteristics of each marker. Notably, high and multi-focal α SMA expression in groups 1, 2, and 3 mice in the acini of the exocrine pancreas was observed. The intensity of α SMA expression was higher in group 2 and 3 than group 1 mice (**Fig. 4C**). Overall cancer marker expression was similar for each animal in the group. In summary, group 1 mice (B6. AAV-SpCas9, AAV-sgRNAs) did not develop pancreatic cancer, but group 2 (B6-SpCas9, AAV-sgRNAs) and group 3 (FVB, AAV-CjCas9-sgRNAs) mice developed early stage of PanIN. Cancer lesion seemed to be detectable after 6 months of AAV-CRISPR transduction, and this is similar to previous reports [29].

DISCUSSION

Pancreatic cancer is the most lethal cancer type, but very few PDAC animal models have been reported for studying its mechanism and therapy. Because multiple gene mutations must occur for developing pancreatic adenocarcinoma, it is nearly impossible to generate an appropriate model by embryo manipulation. Alternatively, *in vivo* gene edited cancer models may serve as fundamental platforms for studying not only early stage neoplasia development and progression in gene levels, but also stromal environmental and immune response [15]. In this study, we present *in vivo* gene editing mediated PanIN development in WT and cas9 overexpression mice, using SpCas9 and CjCas9, respectively.

For *in vivo* gene editing, AAVs are currently the leading candidates for virus-based gene manipulation because of their broad tissue tropism, non-pathogenic nature, and low immunogenicity [30]. Although AAV6 exhibited high pancreatic tropism [31], we applied AAV2 for *in vivo* CRISPR delivery to establish animal model for early stage neoplasia development. As AAV solution was injected via common bile ductal route, local and high transduction only in the pancreatic ductal area was expected. However, a multifocal and diffuse pattern of AAV transduction was observed in AAV-GFP experiment and α SMA expression. Considering that pancreatic cancer originates from the acini or duct in most cases [32], this would be helpful for developing multi-focal pancreatic neoplasia, which has high relevance in human pancreatic cancer.

SpCas9 has simple PAM (5'-NGG-3') and develops a relatively higher DSB frequency than other CRISPR orthologues that have been previously reported for *in vivo* cancer modeling utilizing SpCas9 orthologues [12,15,16,17,29]. In this study, we also applied SpCas9 for DSB formation for the selected targets. With the AAV cargo capacity limitation, we needed to utilize three different AAVs for five targets, and expected tri-co-transduction in single cells; however, no evidence exists for pancreatic cancer development in group 1 mice. Like the previous study, SpCas9 overexpression mice with two AAV groups developed PanIN, suggesting that SpCas9 overexpression mice seemed to be a necessary factor for successful *in vivo* gene editing-mediated disease modeling. Even though mice are commonly utilized for cancer research, genetic distance with humans causes pathological difference such as in the case of *Apc*^{Min} [33]. Thus, *in vivo* gene editing with a mid-sized animal could be an alternative, but only simple knock-out or transgenic mid-sized animals have been produced as cancer models [34]. For versatile application, we tried to evaluate a small-sized Cas9 orthologue, which does not need a transgenic animal, for *in vivo* cancer modeling with a WT animal. The overall cancer progression seemed to be slower in CjCas9 (group 3) than SpCas9 (group

2), but indel frequency was relatively high in CjCas9. Indeed, AAV-all-in-one CjCas9 could develop simultaneous DSB formation for 3 different targets, and this suggests that CjCas9 could be applicable for *in vivo* gene editing including mid-sized WT animals.

For *in vivo* cancer development, we selected five target genes: *Kras*^{G12D}, *Trp53*, *Smad4*, *Brca2*, and *Ink4a*. According to previous reports, the gain of function of *Kras* gene mutation initiate neoplasm formation and was observed in more than 90% of pancreatic cancer patients [35], and *Trp53* and *Ink4a* exhibited relatively high mutation rate than *Smad4* and *Brca2* [18]. Even mutation of each candidate genes enrolled in specific PanIN stage, we tried to develop simultaneous multiplex gene mutation for avoiding multiple surgery for AAV transduction. AAV-SpCas9 and AAV-CjCas9 developed PanIN, but there is no evidence of metastasis and overall progression is slower than previous *in vivo* pancreatic cancer modeling [17,29]. The reason for the slow PanIN development is still uncertain, but the transduction with lower AAV particles number than other studies and the low frequency of *Kras*^{G12D} would cause this. In addition, the influence of transduction route on slow PanIN development could not be confirmed, whether common bile duct or direct pancreatic injection, but unexpectedly, ductal injection developed slower and early grade PanIN than direct pancreatic injection [15,17,29]. However, there were several findings such as 1) multiple DSB potential of AAV-CjCas9, 2) peri-ductal lymphocyte infiltration in every groups, 3) multi-focal cancer marker expression with AAV mediated gene editing, and 4) need more than 12 months for developing initiation of PanIN in AAV mediated targeting.

In this study, we analyzed the subjects for 12 months from AAV-transduction; thus, further progression was not evaluated. In addition, we did not compare the efficiency of *in vivo* editing for other AAV serotypes, lipid nanoparticle or other delivery tools [36]. However, slow cancer development without remarkable symptom would have relevance with human PDAC. In conclusion, *in vivo* gene editing furnished fundamental knowledge for cancer biology and insights into further gene therapy. We have developed an *in vivo* gene editing-based pancreatic cancer model utilizing SpCas9 and CjCas9, and the animals presented PanIN lesions and other aforementioned characteristics. Notably, CjCas9 exhibited high DSB potential for multiple targets, and it is advantageous for *in vivo* gene editing on WT.

SUPPLEMENTARY MATERIALS

Supplementary Table 1

Sequences of sgRNA in this study

[Click here to view](#)

Supplementary Table 2

Summary of *in vivo* gene targeting group

[Click here to view](#)

Supplementary Table 3

Primer sequences used in this study

[Click here to view](#)

Supplementary Fig. 1

Brief targeting map for DSB formation and *Kras*^{G12D} mutation. For loss of function development in various target genes, single sgRNA applied in *Trp53*, *Brca2*, and *Smad4*, but dual sgRNA applied in *Ink4a* for preventing protein synthesis by alternative splicing. In *Kras*^{G12D} generation with SpCas9, one sgRNA were selected, and HDR template with G12D and two silent mutation was incorporated. While in CjCas9 for *Kras*^{G12D}, two sgRNAs applied, and nine silent mutation was incorporated in the HDR template. Red alphabet: target site for 12th exon (pG12D), red bar: PAM sequence with 5'-NGG-3' or 5'-NNNNRYAC-3'. Blue alphabet: silent mutation.

[Click here to view](#)

Supplementary Fig. 2

AAV2 tropism evaluation in pancreas by AAV2-GFP injection. 1.29×10^{10} MOI of AAV-GFP were injected into common bile duct, and GFP expression was confirmed after three weeks and seven weeks. Diffuse and multifocal GFP expression was observed in whole region of pancreas after three weeks from AAV-GFP transduction. In seven weeks after AAV-GFP transduction, spot number of GFP expression decreased and weaken.

[Click here to view](#)

Supplementary Fig. 3

Microscopic analysis on pancreas. Histological images of mesentery lymph node in group2 and group 3 (40×). The black squares are the image range of (B) (12 months, group 2 and 3).

[Click here to view](#)

REFERENCES

1. Ryan DP, Hong TS, Bardeesy N. Pancreatic adenocarcinoma. *N Engl J Med* 2014;371:1039-1049.
[PUBMED](#) | [CROSSREF](#)
2. Bardeesy N, DePinho RA. Pancreatic cancer biology and genetics. *Nat Rev Cancer* 2002;2:897-909.
[PUBMED](#) | [CROSSREF](#)
3. Waddell N, Pajic M, Patch AM, Chang DK, Kassahn KS, Bailey P, Johns AL, Miller D, Nones K, Quek K, Quinn MC, Robertson AJ, Fadlullah MZ, Bruxner TJ, Christ AN, Harliwong I, Idrisoglu S, Manning S, Nourse C, Nourbakhsh E, Wani S, Wilson PJ, Markham E, Cloonan N, Anderson MJ, Fink JL, Holmes O, Kazakoff SH, Leonard C, Newell F, Poudel B, Song S, Taylor D, Waddell N, Wood S, Xu Q, Wu J, Pinese M, Cowley MJ, Lee HC, Jones MD, Nagrial AM, Humphris J, Chantrell LA, Chin V, Steinmann AM, Mawson A, Humphrey ES, Colvin EK, Chou A, Scarlett CJ, Pinho AV, Giry-Laterriere M, Rooman I, Samra JS, Kench JG, Pettitt JA, Merrett ND, Toon C, Epari K, Nguyen NQ, Barbour A, Zeps N, Jamieson NB, Graham JS, Niclou SP, Bjerkvig R, Grützmann R, Aust D, Hruban RH, Maitra A, Iacobuzio-Donahue CA, Wolfgang CL, Morgan RA, Lawlor RT, Corbo V, Bassi C, Falconi M, Zamboni G, Tortora G, Tempero MA, ; Australian Pancreatic Cancer Genome Initiative Gill AJ, Eshleman JR, Pilarsky C, Scarpa A, Musgrove EA, Pearson JV, Biankin AV, Grimmond SM. Whole genomes redefine the mutational landscape of pancreatic cancer. *Nature* 2015;518:495-501.
[PUBMED](#) | [CROSSREF](#)
4. Hruban RH, Adsay NV, Albores-Saavedra J, Compton C, Garrett ES, Goodman SN, Kern SE, Klimstra DS, Klöppel G, Longnecker DS, Lüttges J, Offerhaus GJ. Pancreatic intraepithelial neoplasia: a new nomenclature and classification system for pancreatic duct lesions. *Am J Surg Pathol* 2001;25:579-586.
[PUBMED](#) | [CROSSREF](#)
5. Behrens D, Walther W, Fichtner I. Pancreatic cancer models for translational research. *Pharmacol Ther* 2017;173:146-158.
[PUBMED](#) | [CROSSREF](#)

6. Herreros-Villanueva M, Hijona E, Cosme A, Bujanda L. Mouse models of pancreatic cancer. *World J Gastroenterol* 2012;18:1286-1294.
[PUBMED](#) | [CROSSREF](#)
7. Gopinathan A, Morton JP, Jodrell DI, Sansom OJ. GEMMs as preclinical models for testing pancreatic cancer therapies. *Dis Model Mech* 2015;8:1185-1200.
[PUBMED](#) | [CROSSREF](#)
8. Jinek M, Chylinski K, Fonfara I, Hauer M, Doudna JA, Charpentier E. A programmable dual-RNA-guided DNA endonuclease in adaptive bacterial immunity. *Science* 2012;337:816-821.
[PUBMED](#) | [CROSSREF](#)
9. Cong L, Ran FA, Cox D, Lin S, Barretto R, Habib N, Hsu PD, Wu X, Jiang W, Marraffini LA, Zhang F. Multiplex genome engineering using CRISPR/Cas systems. *Science* 2013;339:819-823.
[PUBMED](#) | [CROSSREF](#)
10. Feng W, Jasin M. Homologous recombination and replication fork protection: BRCA2 and more! *Cold Spring Harb Symp Quant Biol* 2017;82:329-338.
[PUBMED](#) | [CROSSREF](#)
11. Sánchez-Rivera FJ, Papagiannakopoulos T, Romero R, Tammela T, Bauer MR, Bhutkar A, Joshi NS, Subbaraj L, Bronson RT, Xue W, Jacks T. Rapid modelling of cooperating genetic events in cancer through somatic genome editing. *Nature* 2014;516:428-431.
[PUBMED](#) | [CROSSREF](#)
12. Platt RJ, Chen S, Zhou Y, Yim MJ, Swiech L, Kempton HR, Dahlman JE, Parnas O, Eisenhaure TM, Jovanovic M, Graham DB, Jhunjhunwala S, Heidenreich M, Xavier RJ, Langer R, Anderson DG, Hacohen N, Regev A, Feng G, Sharp PA, Zhang F. CRISPR-Cas9 knockin mice for genome editing and cancer modeling. *Cell* 2014;159:440-455.
[PUBMED](#) | [CROSSREF](#)
13. Xue W, Chen S, Yin H, Tammela T, Papagiannakopoulos T, Joshi NS, Cai W, Yang G, Bronson R, Crowley DG, Zhang F, Anderson DG, Sharp PA, Jacks T. CRISPR-mediated direct mutation of cancer genes in the mouse liver. *Nature* 2014;514:380-384.
[PUBMED](#) | [CROSSREF](#)
14. Zuckermann M, Hovestadt V, Knobbe-Thomsen CB, Zapatka M, Northcott PA, Schramm K, Belic J, Jones DT, Tschida B, Moriarity B, Largaespada D, Roussel MF, Korshunov A, Reifenberger G, Pfister SM, Lichter P, Kawauchi D, Gronych J. Somatic CRISPR/Cas9-mediated tumour suppressor disruption enables versatile brain tumour modelling. *Nat Commun* 2015;6:7391.
[PUBMED](#) | [CROSSREF](#)
15. Chiou SH, Winters IP, Wang J, Naranjo S, Dudgeon C, Tamburini FB, Brady JJ, Yang D, Grüner BM, Chuang CH, Caswell DR, Zeng H, Chu P, Kim GE, Carpizo DR, Kim SK, Winslow MM. Pancreatic cancer modeling using retrograde viral vector delivery and *in vivo* CRISPR/Cas9-mediated somatic genome editing. *Genes Dev* 2015;29:1576-1585.
[PUBMED](#) | [CROSSREF](#)
16. Maresch R, Mueller S, Veltkamp C, Öllinger R, Friedrich M, Heid I, Steiger K, Weber J, Engleitner T, Barenboim M, Klein S, Louzada S, Banerjee R, Strong A, Stauber T, Gross N, Geumann U, Lange S, Ringelhan M, Varela I, Unger K, Yang F, Schmid RM, Vassiliou GS, Braren R, Schneider G, Heikenwalder M, Bradley A, Saur D, Rad R. Multiplexed pancreatic genome engineering and cancer induction by transfection-based CRISPR/Cas9 delivery in mice. *Nat Commun* 2016;7:10770.
[PUBMED](#) | [CROSSREF](#)
17. Ideno N, Yamaguchi H, Okumura T, Huang J, Brun MJ, Ho ML, Suh J, Gupta S, Maitra A, Ghosh B. A pipeline for rapidly generating genetically engineered mouse models of pancreatic cancer using *in vivo* CRISPR-Cas9-mediated somatic recombination. *Lab Invest* 2019;99:1233-1244.
[PUBMED](#) | [CROSSREF](#)
18. Cicenas J, Kvederaviciute K, Meskinyte I, Meskinyte-Kausiliene E, Skeberdyte A, Cicenas J. KRAS, TP53, CDKN2A, SMAD4, BRCA1, and BRCA2 mutations in pancreatic cancer. *Cancers (Basel)* 2017;9:E42.
[PUBMED](#) | [CROSSREF](#)
19. Kim E, Koo T, Park SW, Kim D, Kim K, Cho HY, Song DW, Lee KJ, Jung MH, Kim S, Kim JH, Kim JH, Kim JS. *In vivo* genome editing with a small Cas9 orthologue derived from *Campylobacter jejuni*. *Nat Commun* 2017;8:14500.
[PUBMED](#) | [CROSSREF](#)
20. Zhu X, Xu Y, Yu S, Lu L, Ding M, Cheng J, Song G, Gao X, Yao L, Fan D, Meng S, Zhang X, Hu S, Tian Y. An efficient genotyping method for genome-modified animals and human cells generated with CRISPR/Cas9 system. *Sci Rep* 2014;4:6420.
[PUBMED](#) | [CROSSREF](#)

21. Hsiau T, Conant D, Rossi N, Maures T, Waite K, Yang J, Joshi S, Kelso R, Holden K, Enzmann BL, Stoner R. Inference of CRISPR edits from sanger trace data. bioRxivorg 2019. Epub ahead of print. doi: 10.1101/251082.
22. Wang D, Tai PW, Gao G. Adeno-associated virus vector as a platform for gene therapy delivery. *Nat Rev Drug Discov* 2019;18:358-378.
[PUBMED](#) | [CROSSREF](#)
23. Long C, Amoasii L, Mireault AA, McAnally JR, Li H, Sanchez-Ortiz E, Bhattacharyya S, Shelton JM, Bassel-Duby R, Olson EN. Postnatal genome editing partially restores dystrophin expression in a mouse model of muscular dystrophy. *Science* 2016;351:400-403.
[PUBMED](#) | [CROSSREF](#)
24. Swiech L, Heidenreich M, Banerjee A, Habib N, Li Y, Trombetta J, Sur M, Zhang F. *In vivo* interrogation of gene function in the mammalian brain using CRISPR-Cas9. *Nat Biotechnol* 2015;33:102-106.
[PUBMED](#) | [CROSSREF](#)
25. Brembeck FH, Schreiber FS, Deramandt TB, Craig L, Rhoades B, Swain G, Grippo P, Stoffers DA, Silberg DG, Rustgi AK. The mutant K-ras oncogene causes pancreatic periductal lymphocytic infiltration and gastric mucous neck cell hyperplasia in transgenic mice. *Cancer Res* 2003;63:2005-2009.
[PUBMED](#)
26. Fujita H, Ohuchida K, Mizumoto K, Nakata K, Yu J, Kayashima T, Cui L, Manabe T, Ohtsuka T, Tanaka M. Alpha-smooth muscle actin expressing stroma promotes an aggressive tumor biology in pancreatic ductal adenocarcinoma. *Pancreas* 2010;39:1254-1262.
[PUBMED](#) | [CROSSREF](#)
27. Kaur S, Kumar S, Momi N, Sasson AR, Batra SK. Mucins in pancreatic cancer and its microenvironment. *Nat Rev Gastroenterol Hepatol* 2013;10:607-620.
[PUBMED](#) | [CROSSREF](#)
28. Panzuto F, Cicchese N, Partelli S, Rinzivillo M, Capurso G, Merola E, Manzoni M, Pucci E, Iannicelli E, Pilozi E, Rossi M, Doglioni C, Falconi M, Delle Fave G. Impact of Ki67 re-assessment at time of disease progression in patients with pancreatic neuroendocrine neoplasms. *PLoS One* 2017;12:e0179445.
[PUBMED](#) | [CROSSREF](#)
29. Doiron B, DeFronzo RA. A novel experimental model for human mixed acinar-ductal pancreatic cancer. *Carcinogenesis* 2018;39:180-190.
[PUBMED](#) | [CROSSREF](#)
30. Kotterman MA, Schaffer DV. Engineering adeno-associated viruses for clinical gene therapy. *Nat Rev Genet* 2014;15:445-451.
[PUBMED](#) | [CROSSREF](#)
31. Quirin KA, Kwon JJ, Alioufi A, Factora T, Temm CJ, Jacobsen M, Sandusky GE, Shontz K, Chicoine LG, Clark KR, Mendell JT, Korc M, Kota J. Safety and efficacy of AAV retrograde pancreatic ductal gene delivery in normal and pancreatic cancer mice. *Mol Ther Methods Clin Dev* 2017;8:8-20.
[PUBMED](#) | [CROSSREF](#)
32. Ferreira RM, Sancho R, Messal HA, Nye E, Spencer-Dene B, Stone RK, Stamp G, Rosewell I, Quaglia A, Behrens A. Duct- and acinar-derived pancreatic ductal adenocarcinomas show distinct tumor progression and marker expression. *Cell Reports* 2017;21:966-978.
[PUBMED](#) | [CROSSREF](#)
33. Jackstadt R, Sansom OJ. Mouse models of intestinal cancer. *J Pathol* 2016;238:141-151.
[PUBMED](#) | [CROSSREF](#)
34. Schachtschneider KM, Schwind RM, Newson J, Kinachtchouk N, Rizko M, Mendoza-Elias N, Grippo P, Principe DR, Park A, Overgaard NH, Jungersen G, Garcia KD, Maker AV, Rund LA, Ozer H, Gaba RC, Schook LB. The oncopig cancer model: an innovative large animal translational oncology platform. *Front Oncol* 2017;7:190.
[PUBMED](#) | [CROSSREF](#)
35. Cicenias J, Tamosaitis L, Kvederaviciute K, Tarvydas R, Staniute G, Kalyan K, Meskinyte-Kausiliene E, Stankevicius V, Valius M. KRAS, NRAS and BRAF mutations in colorectal cancer and melanoma. *Med Oncol* 2017;34:26.
[PUBMED](#) | [CROSSREF](#)
36. Finn JD, Smith AR, Patel MC, Shaw L, Youniss MR, van Heteren J, Dirstine T, Ciullo C, Lescarbeau R, Seitzer J, Shah RR, Shah A, Ling D, Growe J, Pink M, Rohde E, Wood KM, Salomon WE, Harrington WF, Dombrowski C, Strapps WR, Chang Y, Morrissey DV. A single administration of CRISPR/Cas9 lipid nanoparticles achieves robust and persistent *in vivo* genome editing. *Cell Reports* 2018;22:2227-2235.
[PUBMED](#) | [CROSSREF](#)